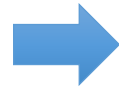
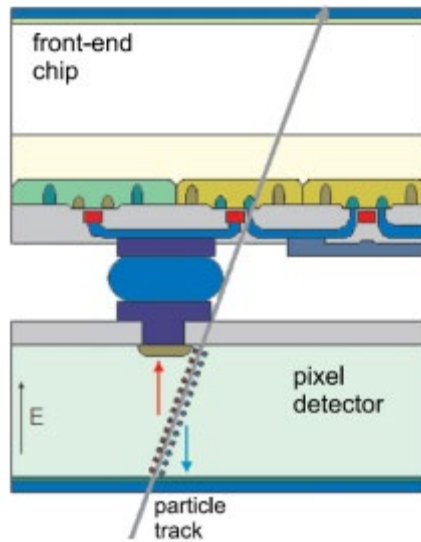


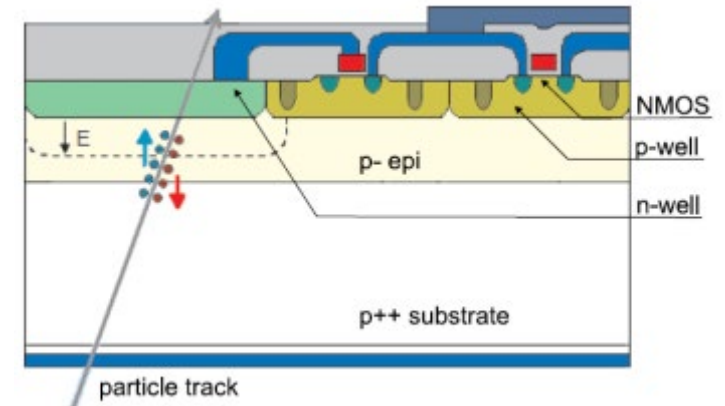
# Rivelatori e Apparati

Slides\_9 – MAPS, DMAPS, LGAD

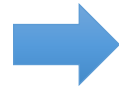
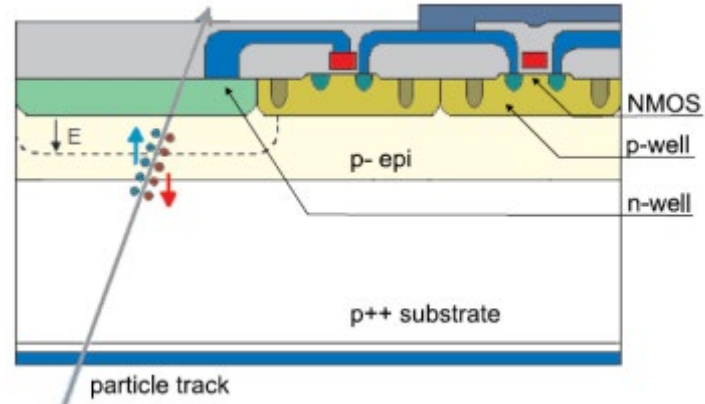
## Hybrid Pixel Detectors



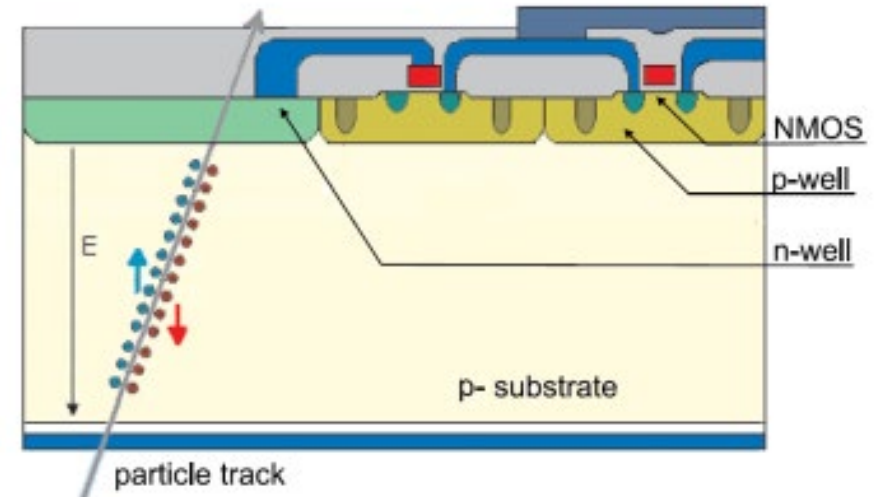
## Monolithic Pixels



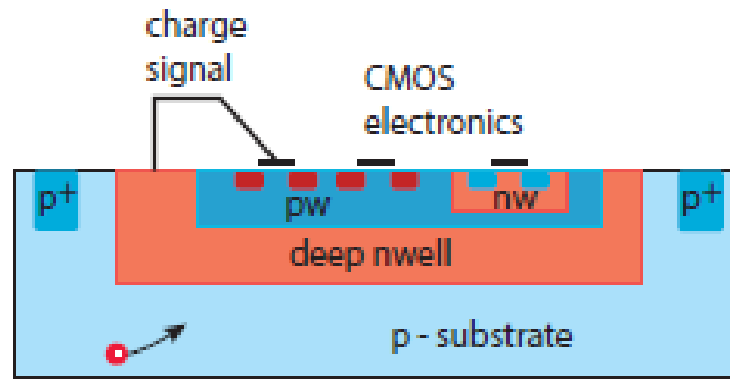
## Monolithic Pixels



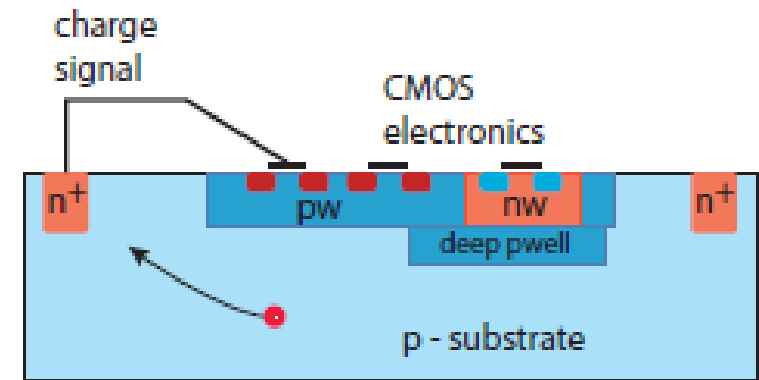
## Depleted Monolithic Pixels



# Fill factor

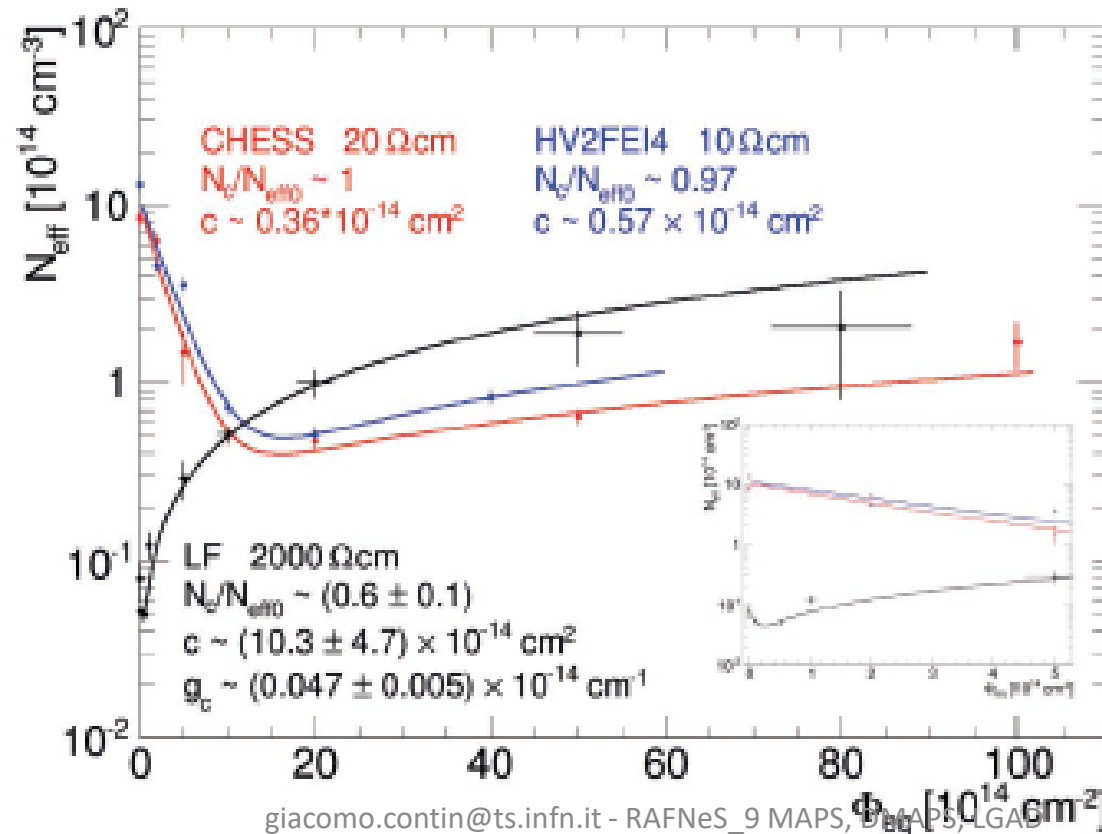


(a) Large fill-factor



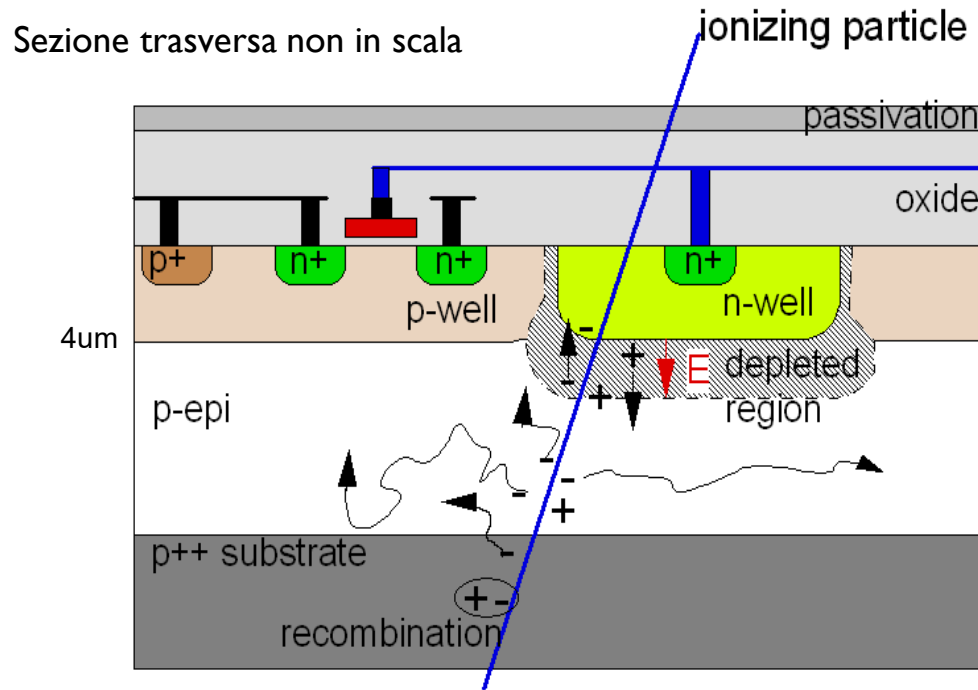
(b) Small fill-factor

# Resistività' substrato



# La tecnologia MAPS

## Volume sensibile e logica CMOS di prima elaborazione del segnale nello stesso cristallo di silicio



- ▶ Monolithic Active Pixel Sensor
- ▶ Tecnologia industriale standard CMOS
- ▶ **Room temperature** operation
- ▶ Sensore e processazione del segnale integrati nello stesso silicio
- ▶ Il segnale e' creato nell'epitassiale (tipicamente  $\sim 10-15 \mu\text{m}$ ) a basso drogaggio  $\rightarrow$  segnale di un MIP limitato a  $< 1000$  elettroni
- ▶ La raccolta di carica avviene soprattutto per diffusione termica (lenta,  $\sim 100 \text{ ns}$ ), anche grazie ai confini "riflettenti" reflective boundaries at p-well and substrate.
- ▶ Epitassiali ad alta resistivita' per ottenere zone svuotate piu' spesse  $\rightarrow$  raccolta della carica piu' efficiente, piu' tollerante alle radiazioni
- ▶ 100% fill-factor

# STAR HFT PXL sensor: Ultimate-2

- ▶ *Ultimate-2*: third generation sensor developed for PXL by the PICSEL group of IPHC, Strasbourg
- ▶ *Monolithic Active Pixel Sensor* technology, MIMOSA series

- **High resistivity p-epi layer**

- Reduced charge collection time
- Improved radiation hardness

- **S/N ~ 30**

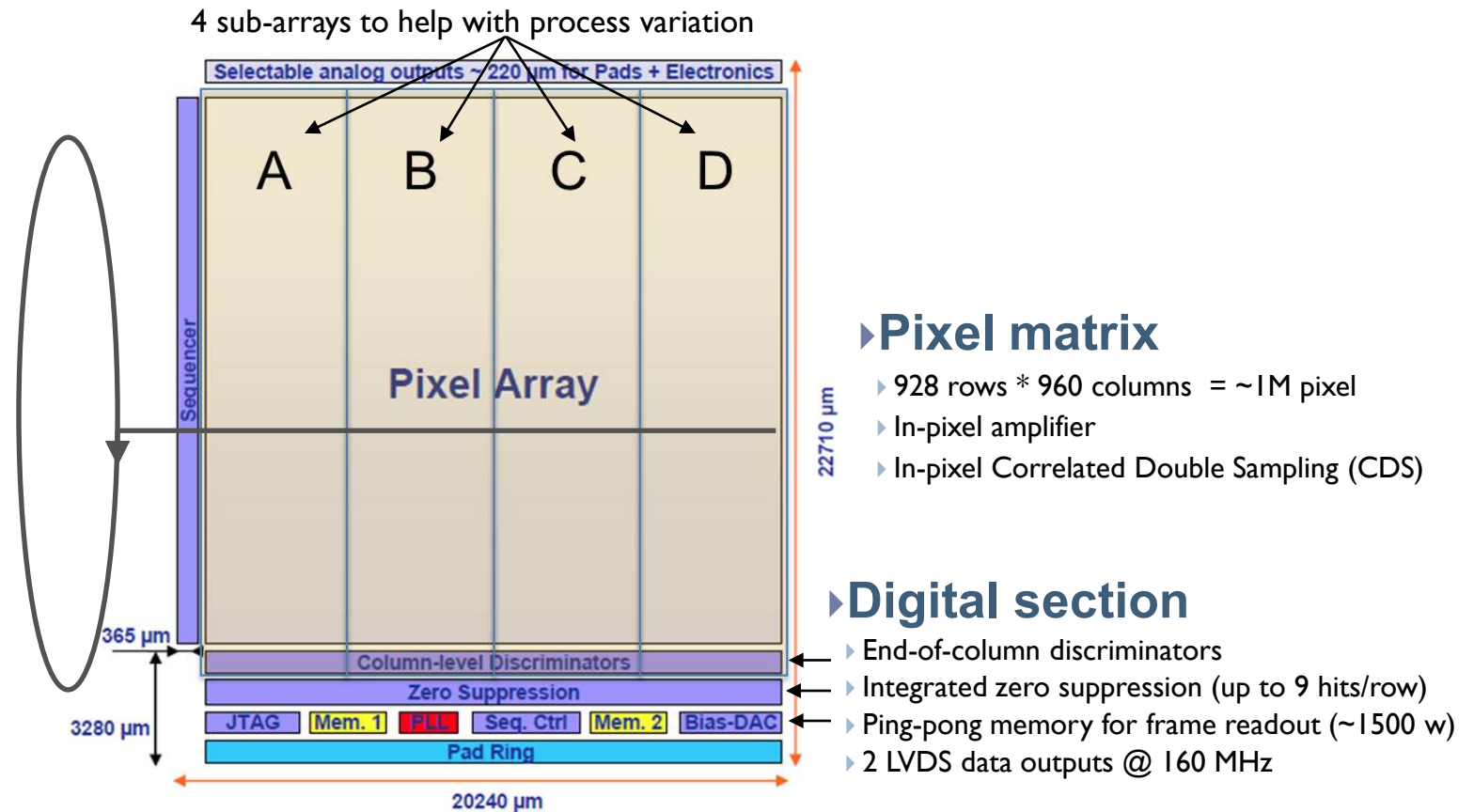
- **MIP Signal ~ 1000 e-**

- **Rolling-shutter readout**

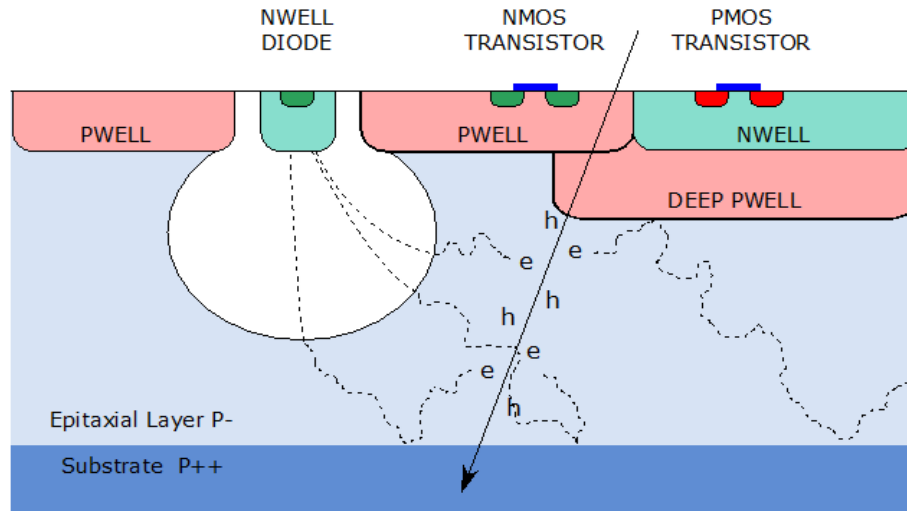
- A row is selected
- For each column, a pixel is connected to discriminator
- Discriminator detects possible hit
- Move to next row

- **185.6  $\mu$ s integration time**

- **~170 mW/cm<sup>2</sup> power dissipation**



## CMOS Pixel Sensor using TowerJazz 0.18 $\mu\text{m}$ CMOS Imaging Process

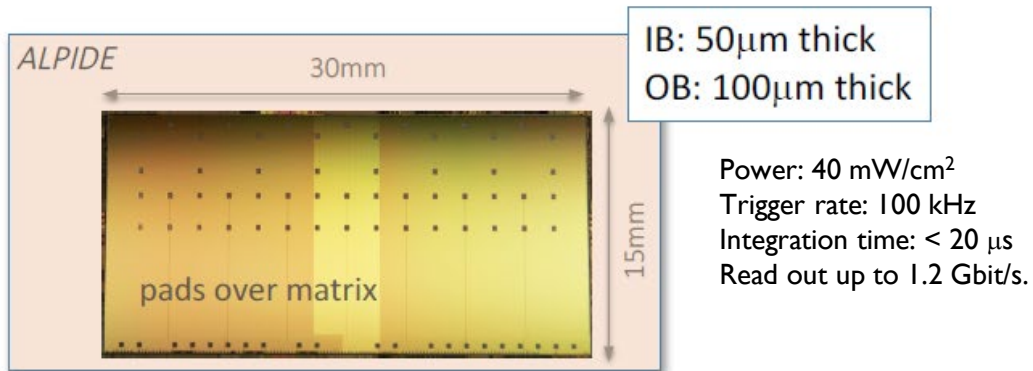
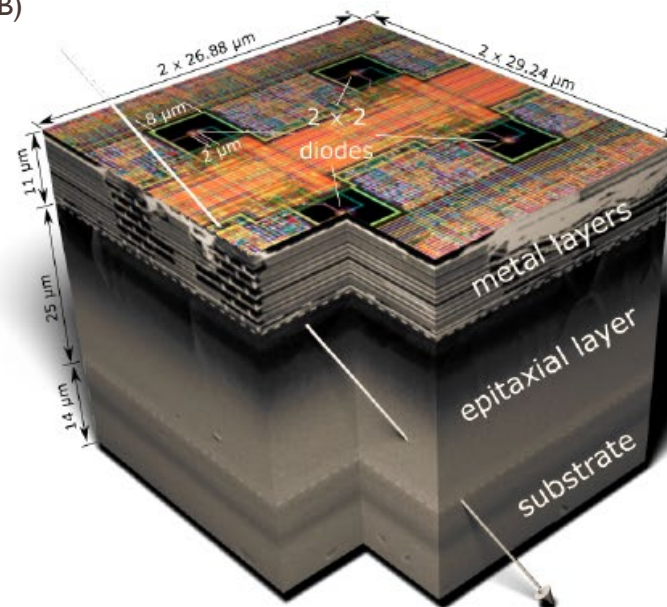
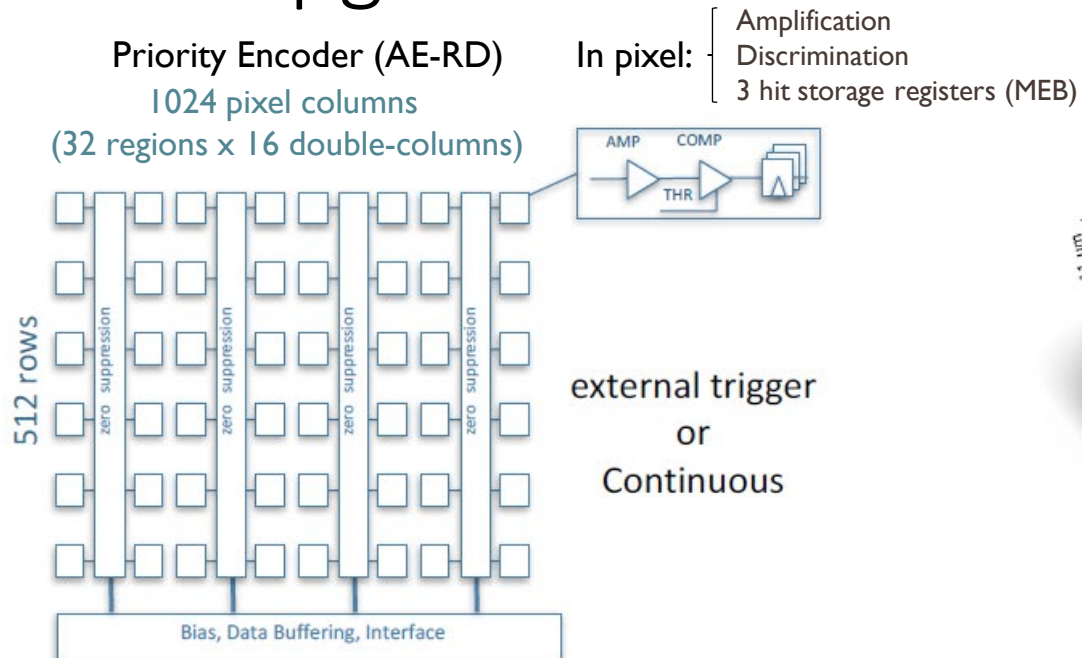


### **ALPIDE** sensor (*developed within ALICE*)

- $\sim 28 \mu\text{m}$  pitch
- Integration time:  $< 20 \mu\text{s}$
- Trigger rate: 100 kHz
- Read out up to 1.2 Gbit/s
- Power: 40 mW/cm<sup>2</sup>
- Priority encoder - sparsified readout
- Rad.Tolerant: 700krad -  $10^{14}$  1MeV  $n_{\text{eq}}/\text{cm}^2$

- ▶ High-resistivity ( $> 1\text{k}\Omega \text{ cm}$ ) p-type epitaxial layer ( $20\mu\text{m} - 40\mu\text{m}$  thick) on p-type substrate
- ▶ Small n-well diode ( $2-3 \mu\text{m}$  diameter),  $\sim 100$  times smaller than pixel  $\Rightarrow$  low capacitance
- ▶ Application of (moderate) reverse bias voltage to substrate can be used to increase depletion zone around NWELL collection diode
- ▶ Quadruple well process: deep PWELL shields NWELL of PMOS transistors, allowing for full CMOS circuitry within active area

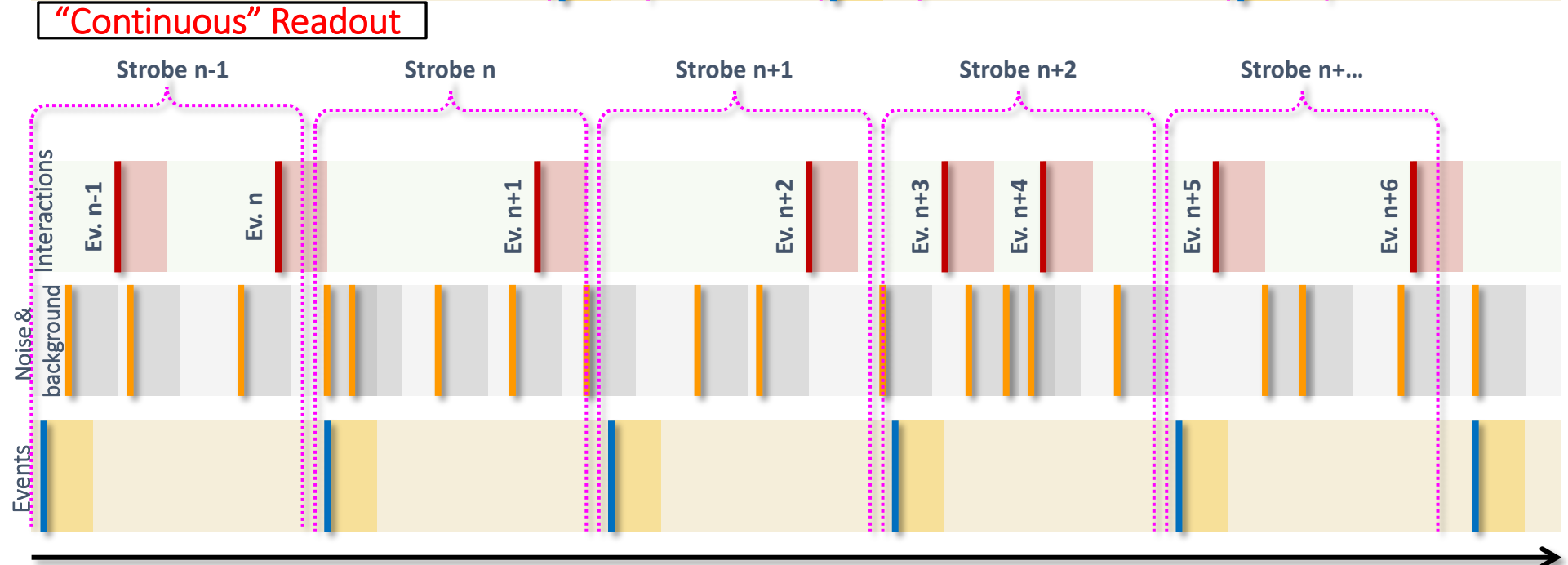
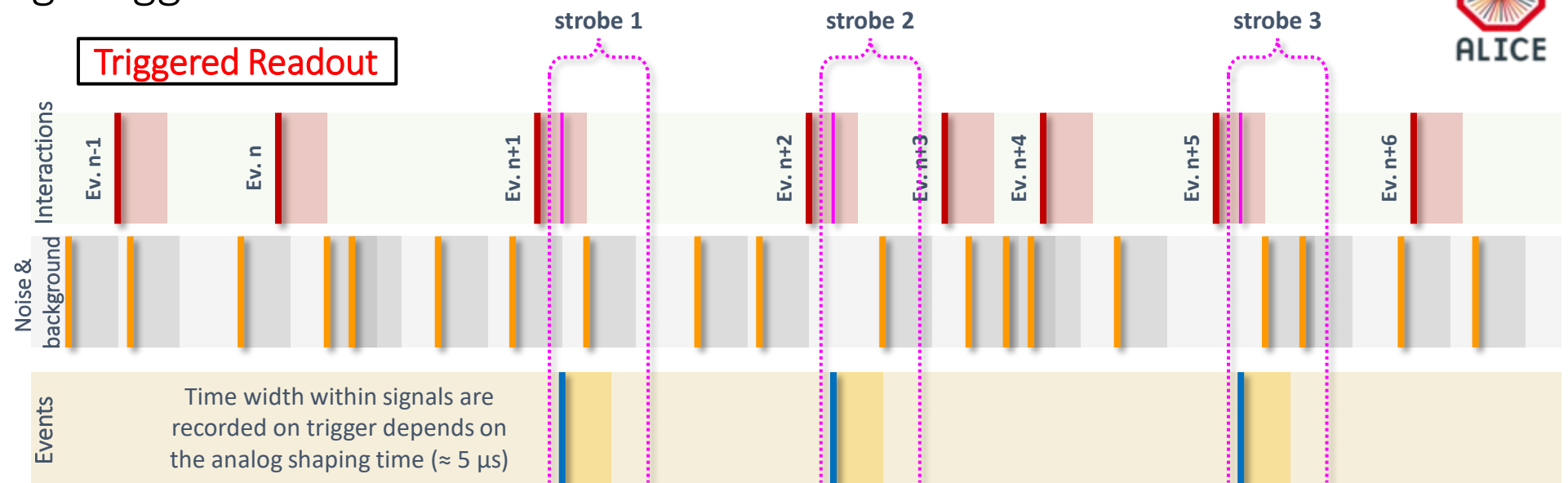
# ALICE ITS Upgrade sensor: ALPIDE



130,000 pixels / cm<sup>2</sup> 27x29x25 μm<sup>3</sup>  
 spatial resolution: ~ 5 μm (3-D)  
 Max particle rate: 100 MHz / cm<sup>2</sup>  
 fake-hit rate: ~ 10<sup>-10</sup> pixel / event  
 power : ~ 300 nW / pixel



# ALPIDE Timing: Triggered & "Continuous" Readout

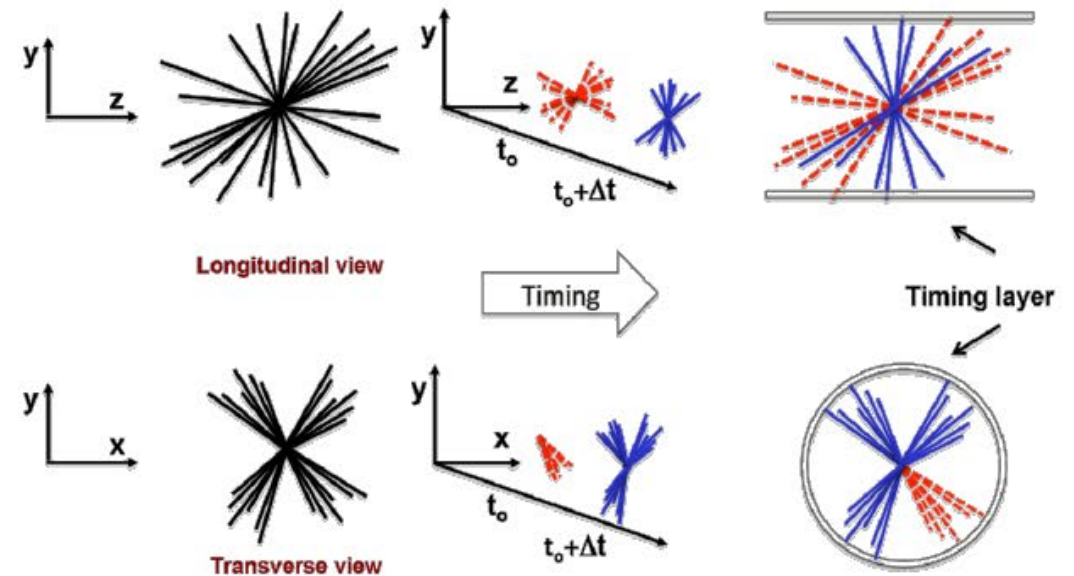
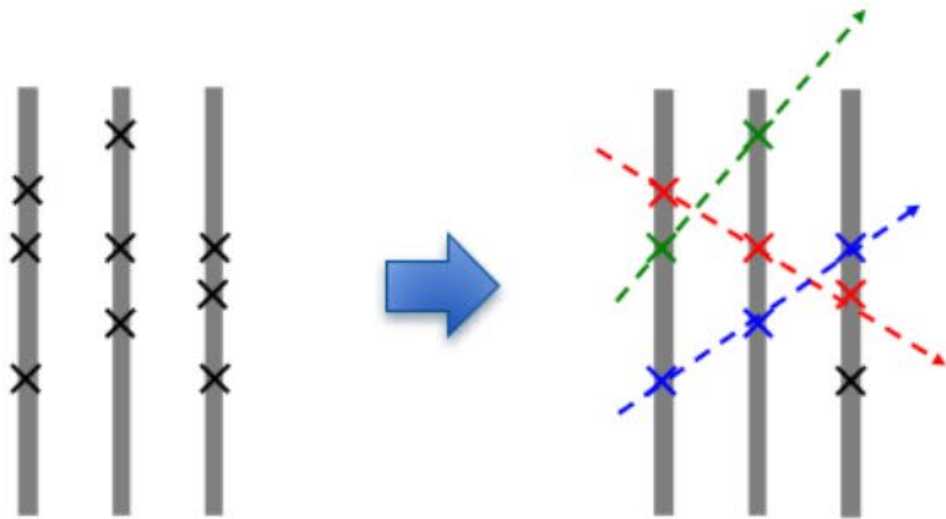


# Rivelatori al silicio per misure di tempo

- Low Gain Avalanche Detectors (LGAD):
  - Rivelatori a valanga a basso guadagno
- SPAD
  - Single-photon avalanche photodiode: fotodiode usato in regime valanga, come un interruttore seguito da una resistenza di quenching che spegne la valanga
- SiPM
  - Silicon Photo-Multiplier: matrici di SPAD in parallelo, non usato per immagine perché somma i segnali dalle diverse celle

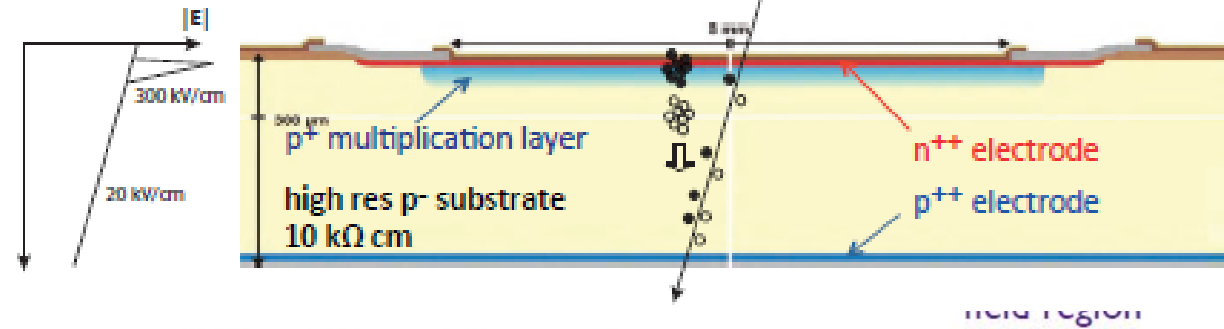
# Acquisition of timing information

- Time tagging at each point
  - LHCb Upgrade II (Run 5 ~2030)
- Timing in the event reconstruction
  - HL-LHC: ATLAS and CMS



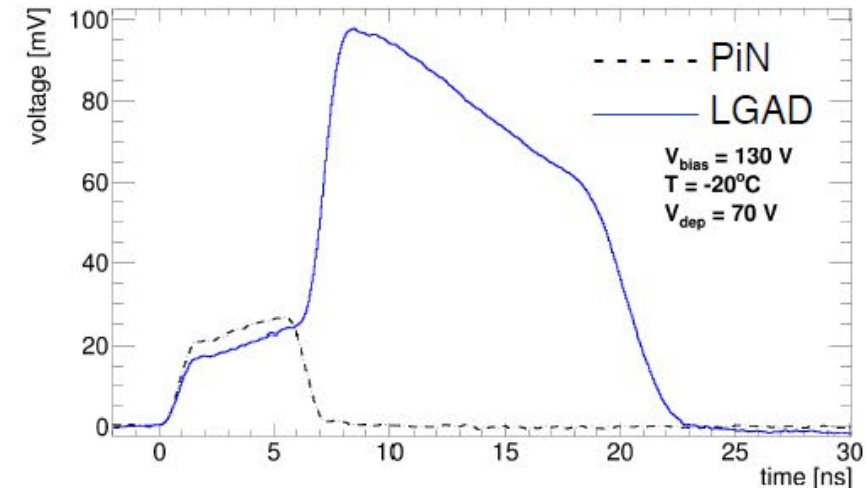
# Gain mechanism in LGADs

- Planar silicon sensors (n+/p/p-)
  - n+ implant, p substrate
  - p-type multiplication layer



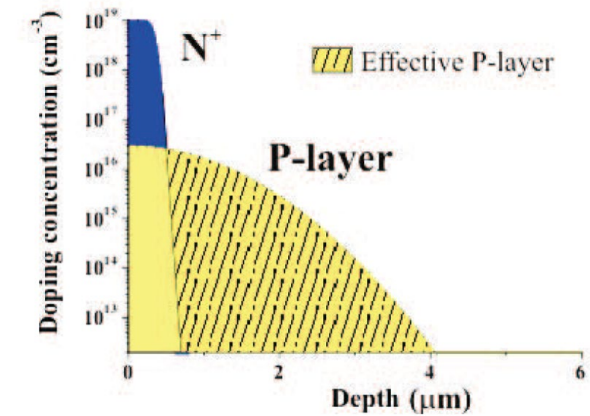
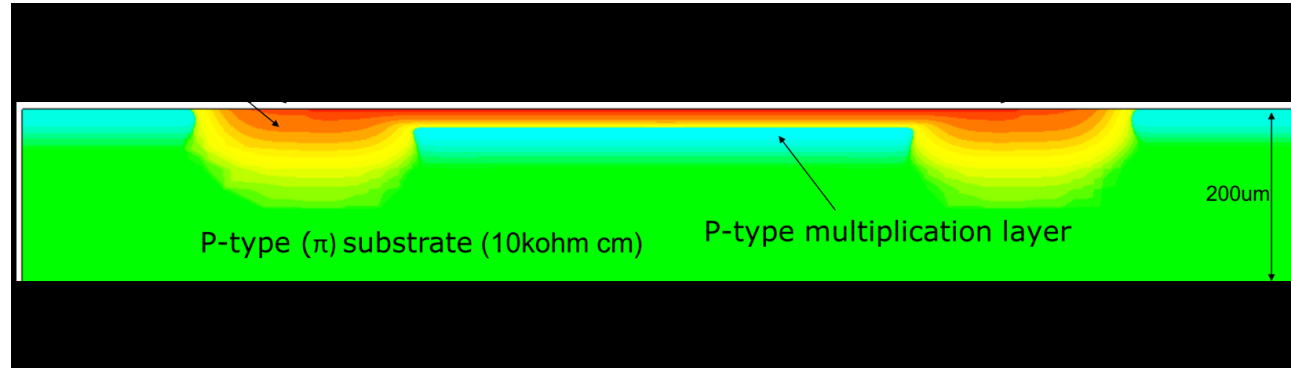
- **High electric field region in the multiplication layer**

- Charges undergo impact ionisation
- Gain depends on:
  - multiplication layer doping
  - bias voltage
  - temperature

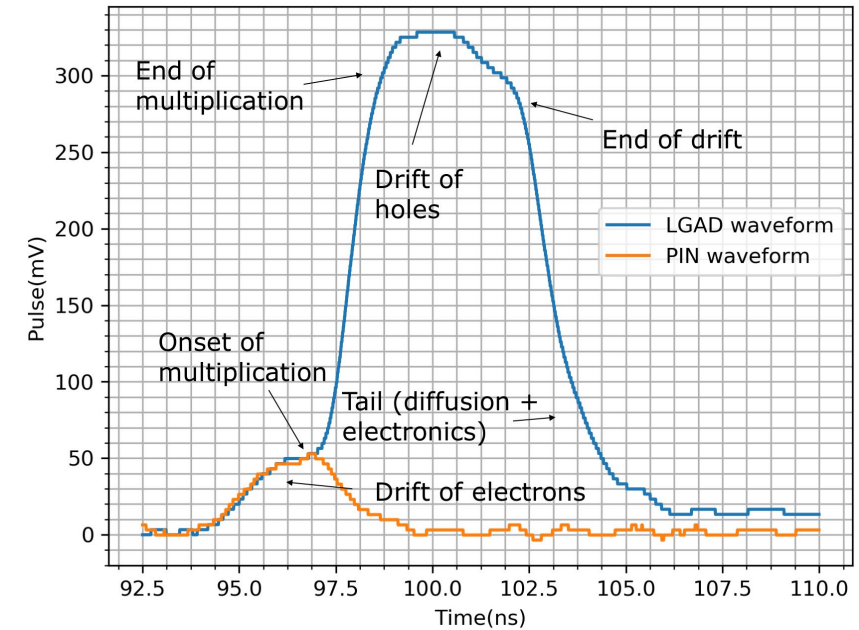
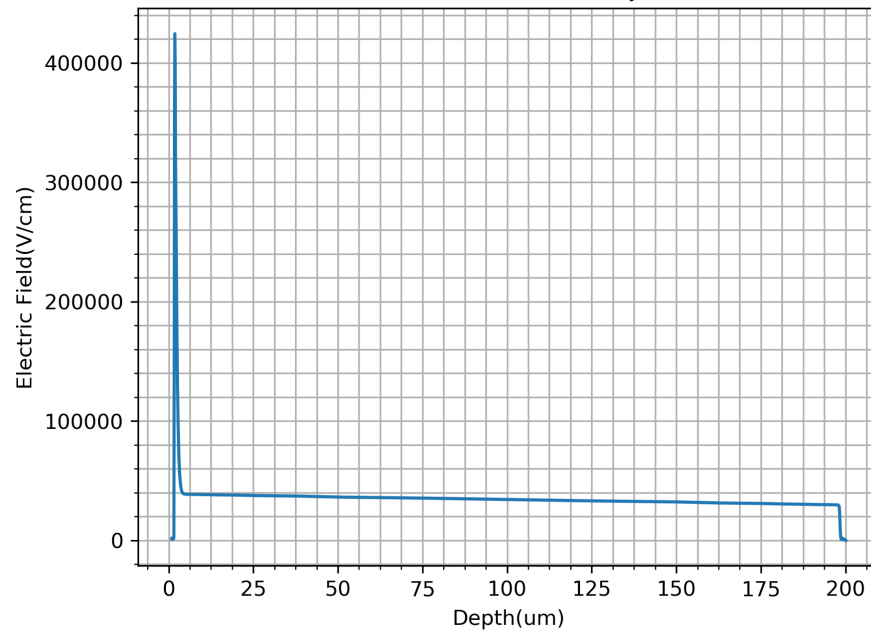


S. Otero Ugobono et al., IEEE TNS (2018) vol. 6, no. 8, pp. 1667-1675

# LGAD: simulazioni

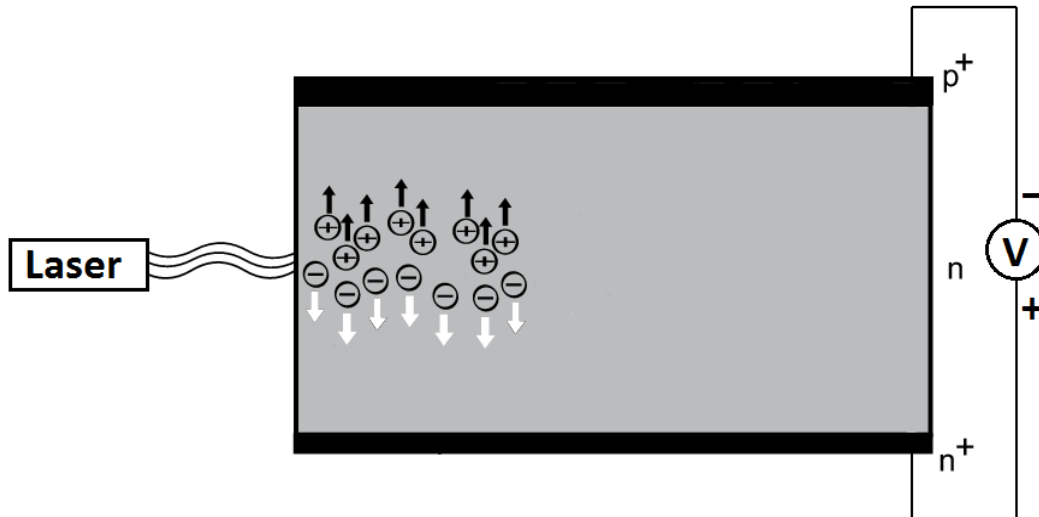


Electric Field Profile across junction

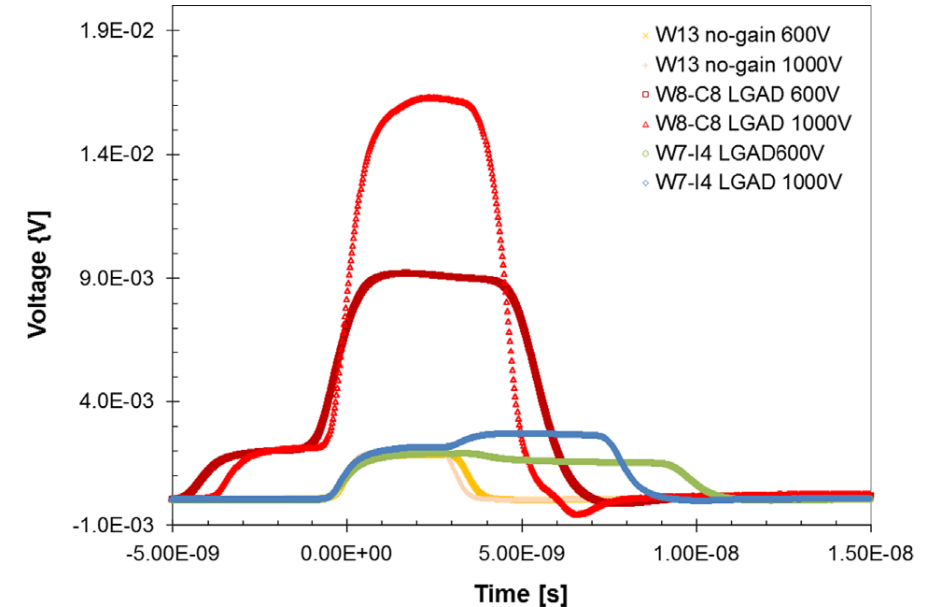


# LGAD: misura TCT

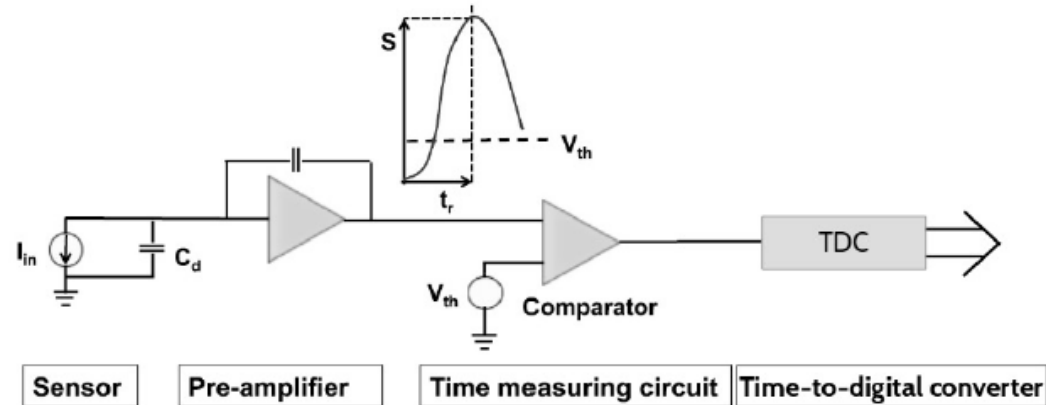
- Principio di funzionamento (Edge-)Transient Current Technique



- Misura TCT su LGAD con diversi Guadagni e a diverse  $V_{bias}$



# Time resolution



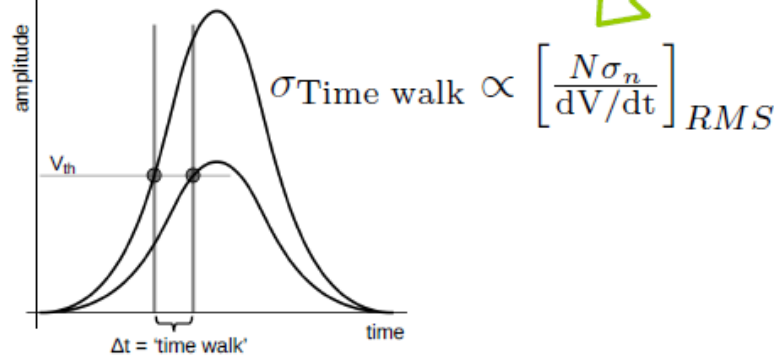
$$\sigma_t^2 = \sigma_{\text{Time walk}}^2 + \sigma_{\text{Landau noise}}^2 + \sigma_{\text{Jitter}}^2 + \sigma_{\text{Distortion}}^2 + \sigma_{\text{TDC}}^2$$

Time resolution is affected by:

- each step in the read-out process
- any effect that changes the shape of the signal

# Time resolution

$$\sigma_t^2 = \sigma_{\text{Time walk}}^2 + \sigma_{\text{Landau noise}}^2 + \sigma_{\text{Jitter}}^2 + \sigma_{\text{Distortion}}^2 + \sigma_{\text{TDC}}^2$$



- Variation in time of arrival due to different signal amplitudes
- Can be compensated by electronics

- Caused by inhomogeneous:
  - drift velocity
  - weighting field
- Solutions:
  - saturated drift velocity
  - optimised geometry

TDC: time-to-digital converter

$$\sigma_{\text{TDC}} = \Delta T / \sqrt{12}$$

comparator  
time bin width

- Sub-picosecond  
⇒ negligible

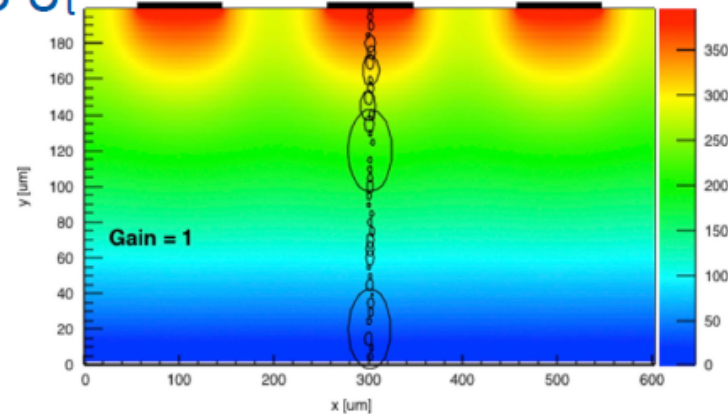
- $V_{th}$ : threshold voltage to determine the time of arrival
- $N\sigma_n$ : the threshold is usually expressed in multiples of the system noise



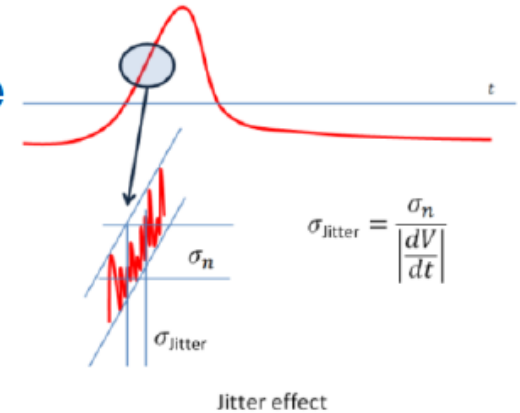
# Time resolution

$$\sigma_t^2 = \sigma_{\text{Time walk}}^2 + \sigma_{\text{Landau noise}}^2 + \sigma_{\text{Jitter}}^2 + \sigma_{\text{Distortion}}^2 + \sigma_{\text{TDC}}^2$$

- Signal shape variations for MIPs
  - Non-uniform energy deposition per unit length
- Sets a physical limit to  $\sigma_t$
- Can be minimised by:
  - setting a low  $V_{\text{th}}$
  - using thin devices



- Variations in time of arrival due to signal noise



- Can be minimised with:
  - low noise sensors
  - low noise electronics
  - fast slew rates

- $V_{\text{th}}$ : threshold voltage to determine the time of arrival



# 4-D Ultra-Fast Si Detectors in pCT



In support of Hadron Therapy, the relative stopping power (RSP) is being reconstructed in 3D.

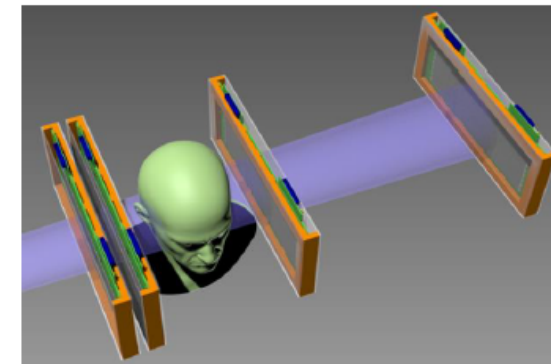
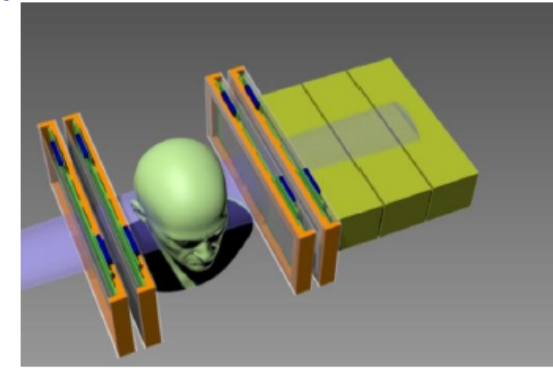
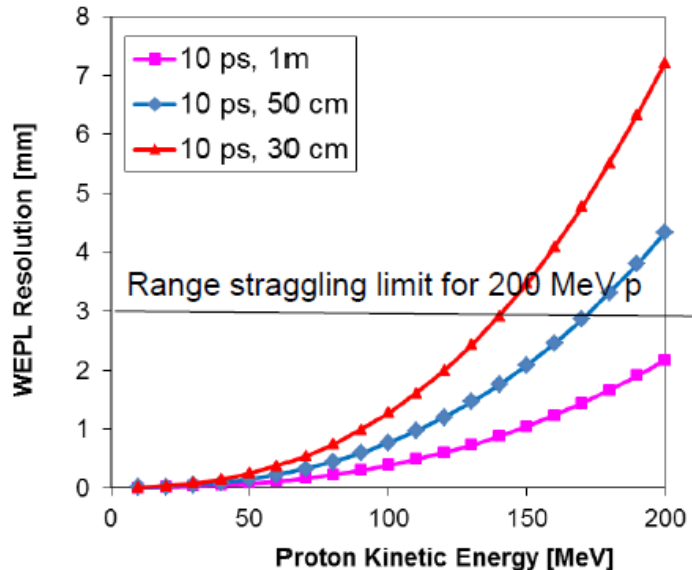
The UCSC-LLU pCT scanner uses Si strip sensors to locate the proton and heavy scintillator stages to measure its energy loss (WEPL).

Protons of 200 MeV have a range of ~ 30 cm in plastic scintillator. The resulting straggling limits the WEPL resolution.



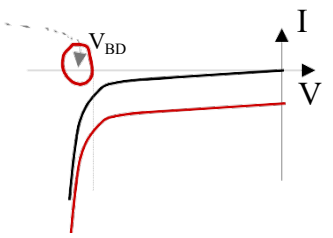
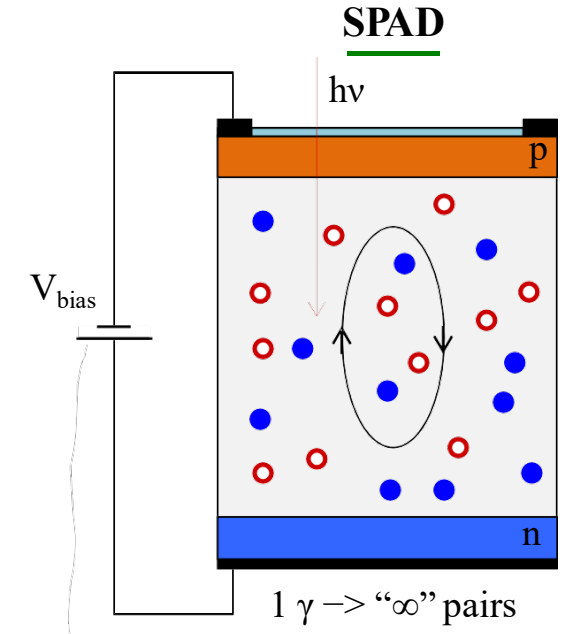
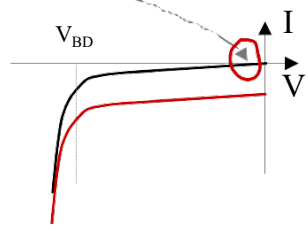
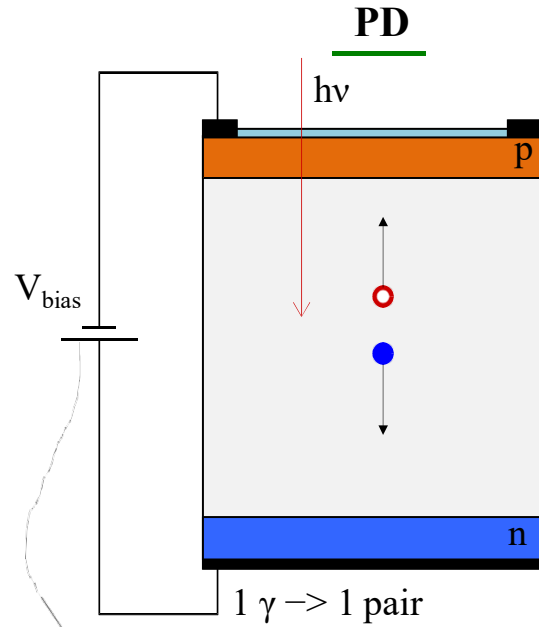
## Replace calorimeter/range counter by UFSD:

Combine tracking with WEPL measurement where the ToF of the proton measures the residual energy., with comparable or better resolution than the scintillator.

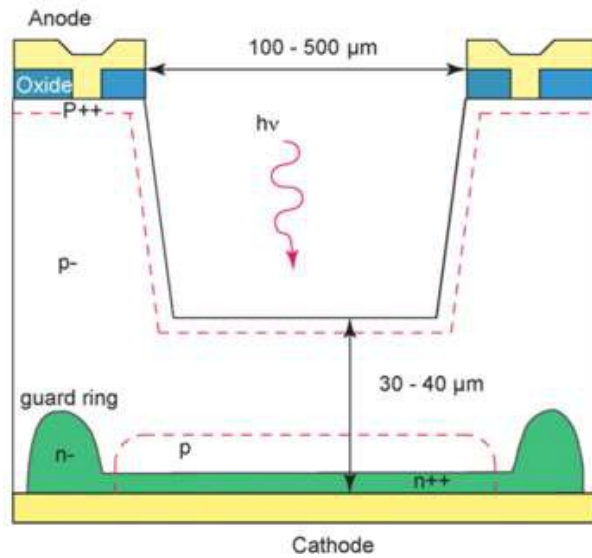


Light-weight,  
all silicon  
construction  
ideal for  
installation  
Into the gantry

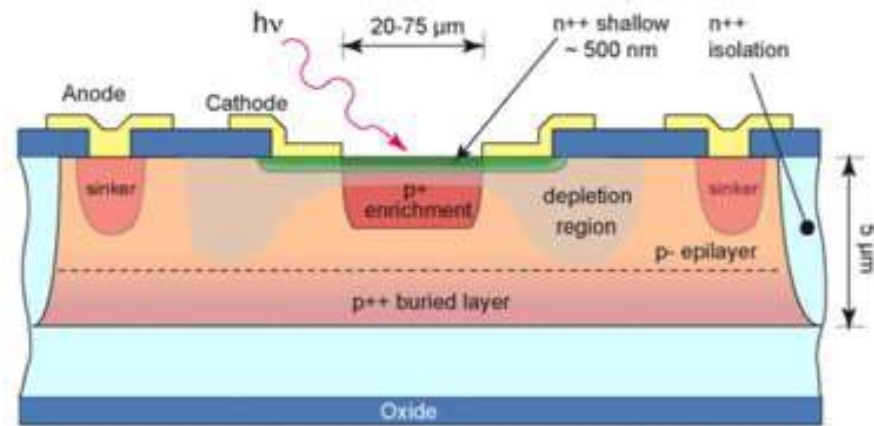
# PD and SPAD



## Structure of a SPAD



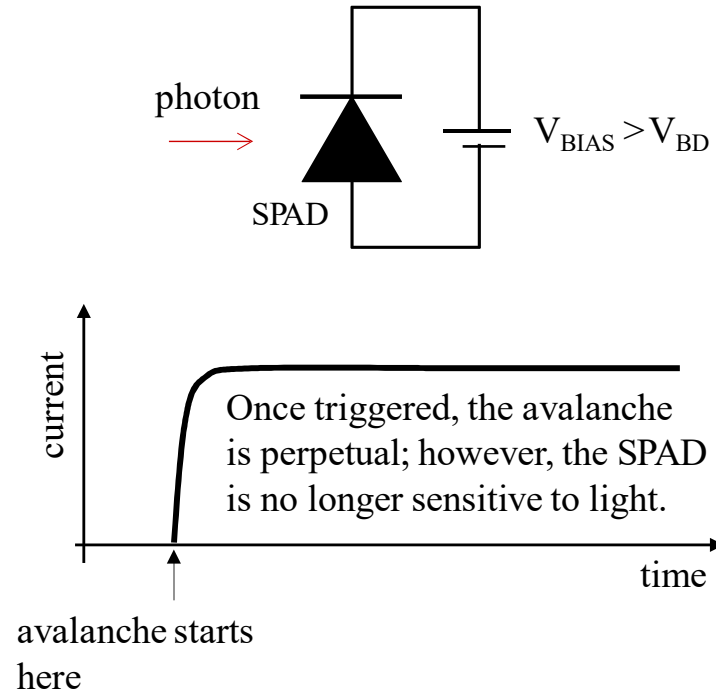
Structure of a *thick* SPAD



Structure of a *thin* SPAD. This structure is used in SPAD arrays.

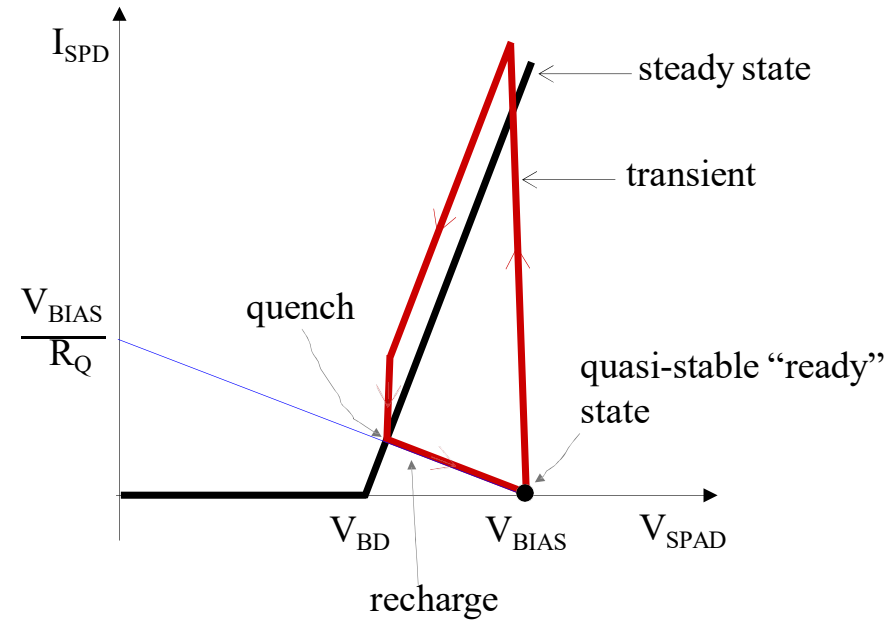
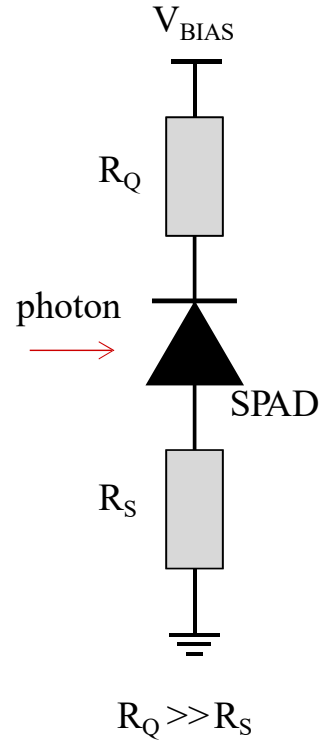
Figures from Zappa et al. 2007

## Operation of a SPAD



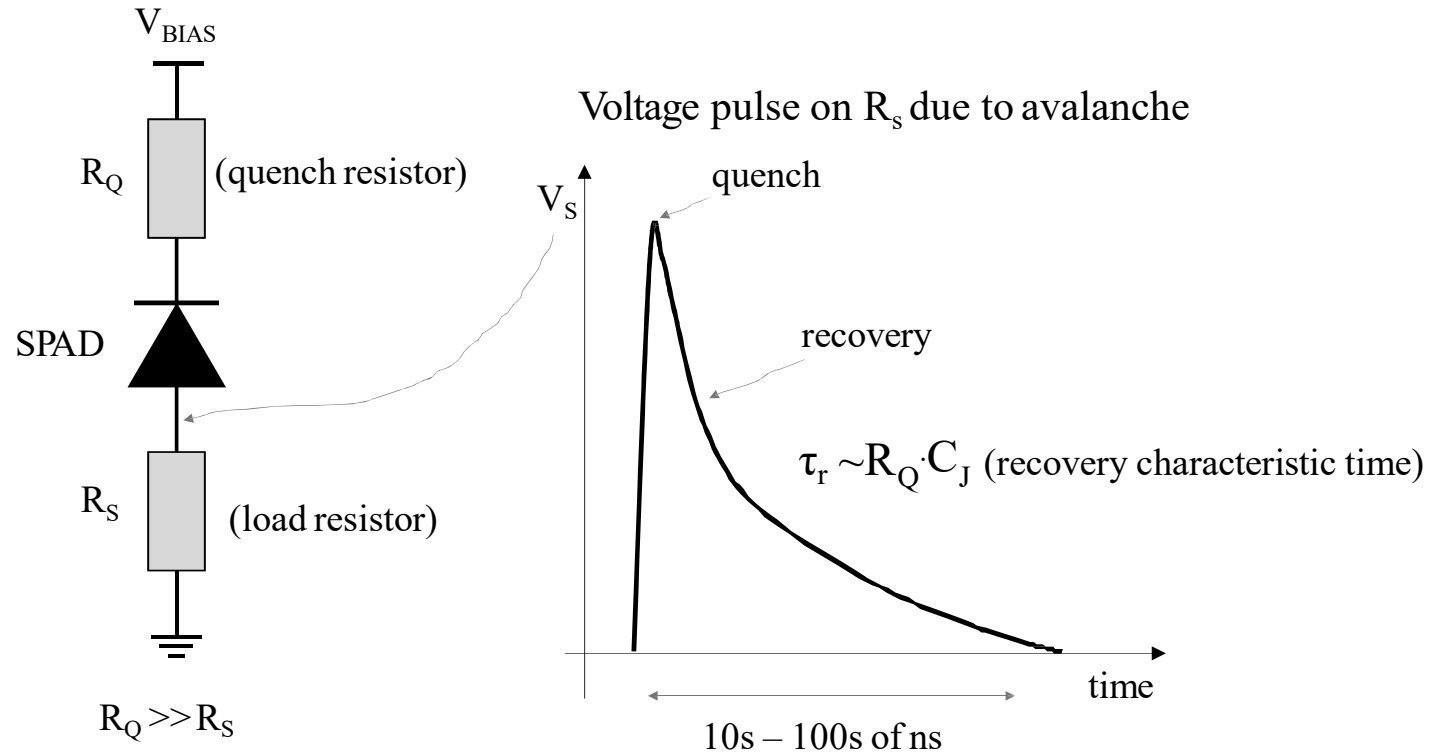
Without quenching, SPAD operates as a light switch.

## Operation of a SPAD (passive quenching)

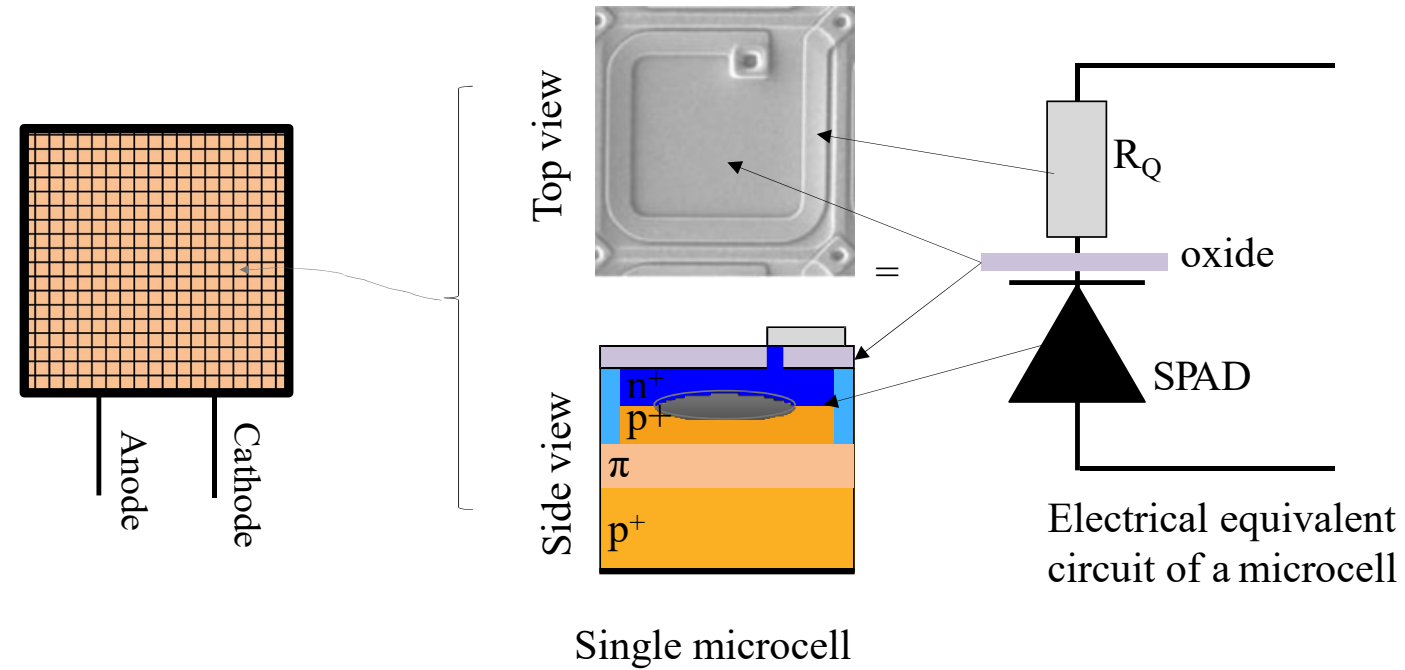


$R_Q$  must be large enough to ensure quenching.

## Operation of SPAD (passive quenching)



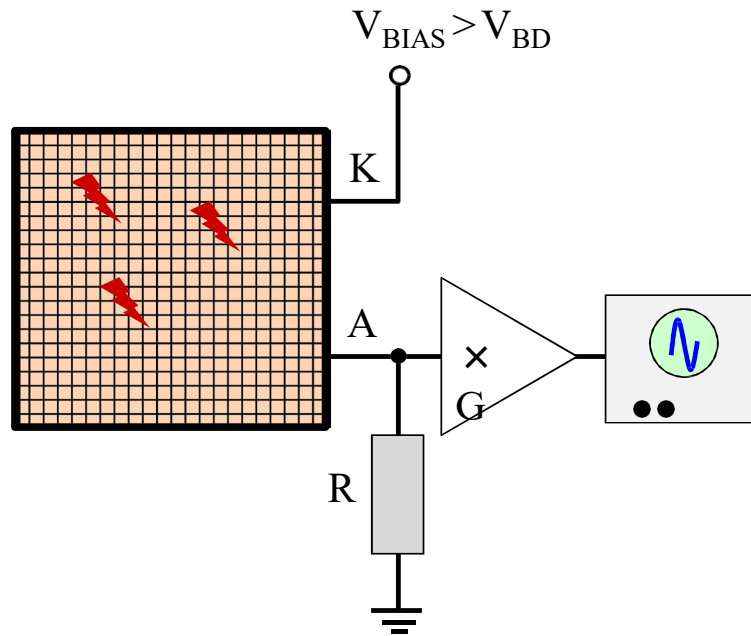
## Si-PM Silicon photomultiplier: structure



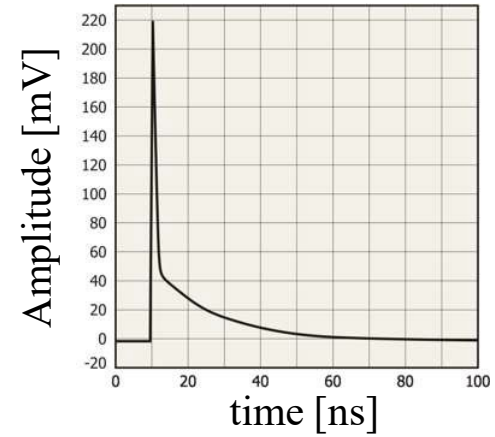
Each microcell is a SPAD in series with a quench resistor. All microcells are connected in parallel. SiPM is **not** an imaging device because all microcells share a common current summing node.



## Silicon photomultiplier: operation



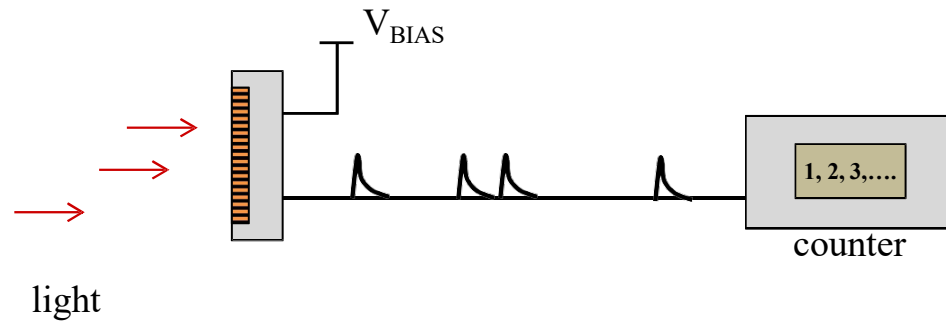
Overvoltage,  $\Delta V = V_{BIAS} - V_{BD}$



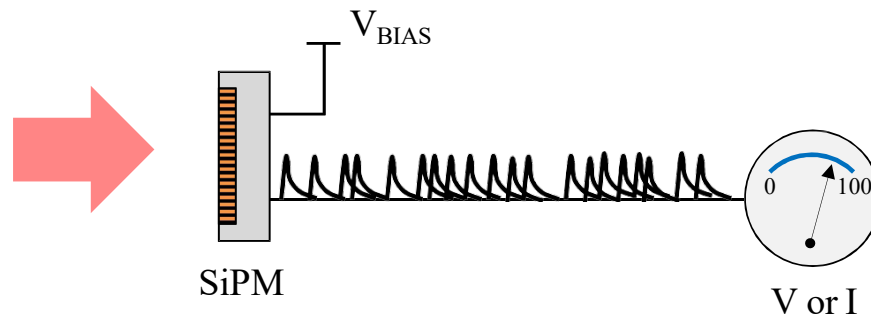
Example of single-photoelectron waveform (1 p.e.)

Gain = area under the curve in electrons

## Silicon photomultiplier: modes of operation



If the pulses are distinguishable, SiPM can be operated in a **photon counting** mode.

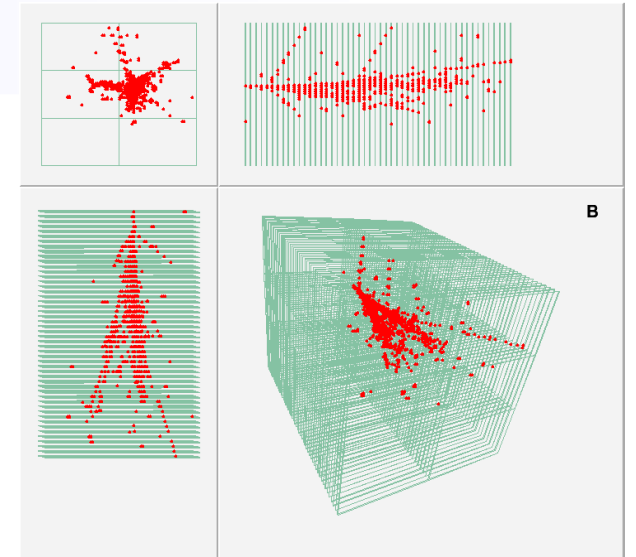
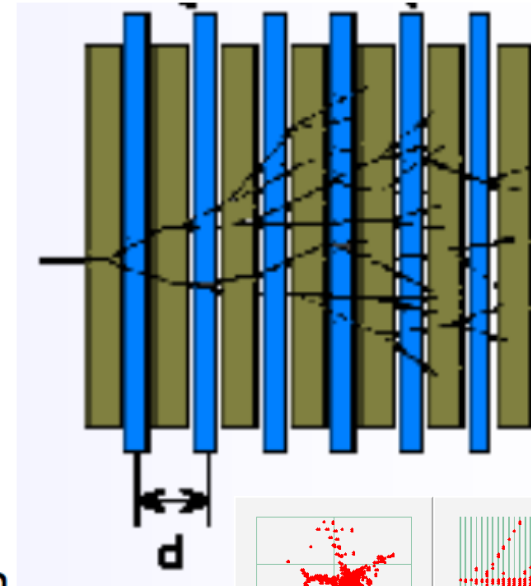


If the pulses overlap, the SiPM can be operated in an **analog mode**. The measured output is voltage or current.

- Applicazione rivelatori al silicio in calorimetria:
  - Calorimetri a campionamento

# Sampling calorimeters

- Use different media
  - High density absorber
  - Interleaved with active readout devices
  - Most commonly used: sandwich structures →
  - But also: embedded fibres, .....
- Sampling fraction
  - $f_{\text{sampl}} = E_{\text{visible}} / E_{\text{total deposited}}$
- Advantages:
  - Cost, transverse and longitudinal segmentation
- Disadvantages:
  - Only part of shower seen, less precise

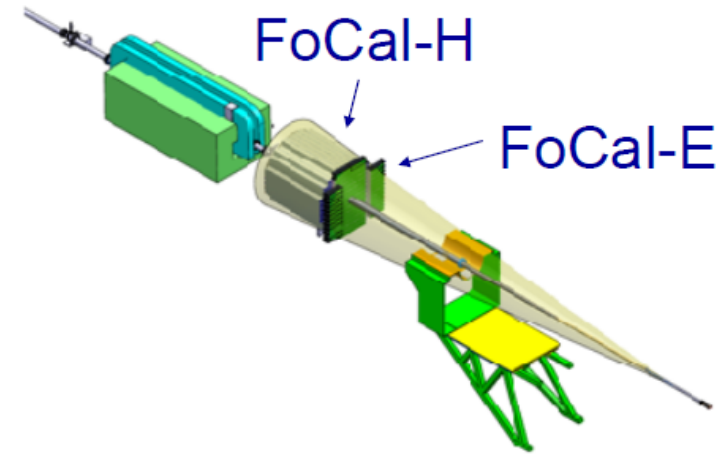


# The FoCal proposal

$3.2 < \eta < 5.8$   
(baseline design @ 7m)

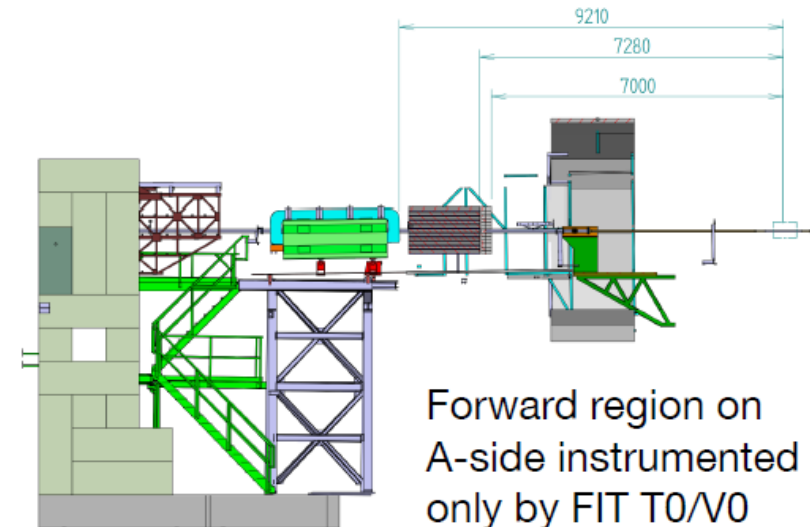
**FoCal-E:** high-granularity Si-W sampling calorimeter for photons and  $\pi^0$

**FoCal-H:** conventional Cu-Sc sampling calorimeter for photon isolation and jets

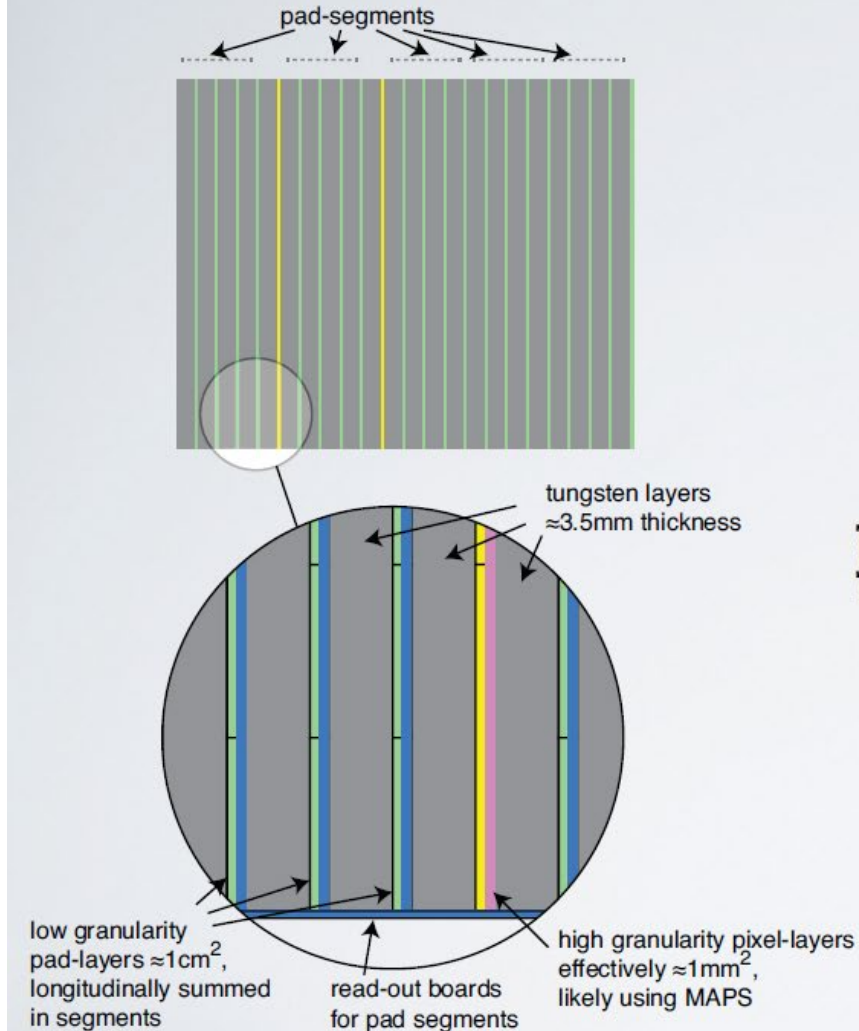


Observables:

- $\pi^0$  (and other neutral mesons)
- Isolated photons
- Jets (and di-jets)
- $J/\psi$  ( $\Upsilon$ ) in UPC
- W, Z
- Event plane and centrality



# Strawman Design

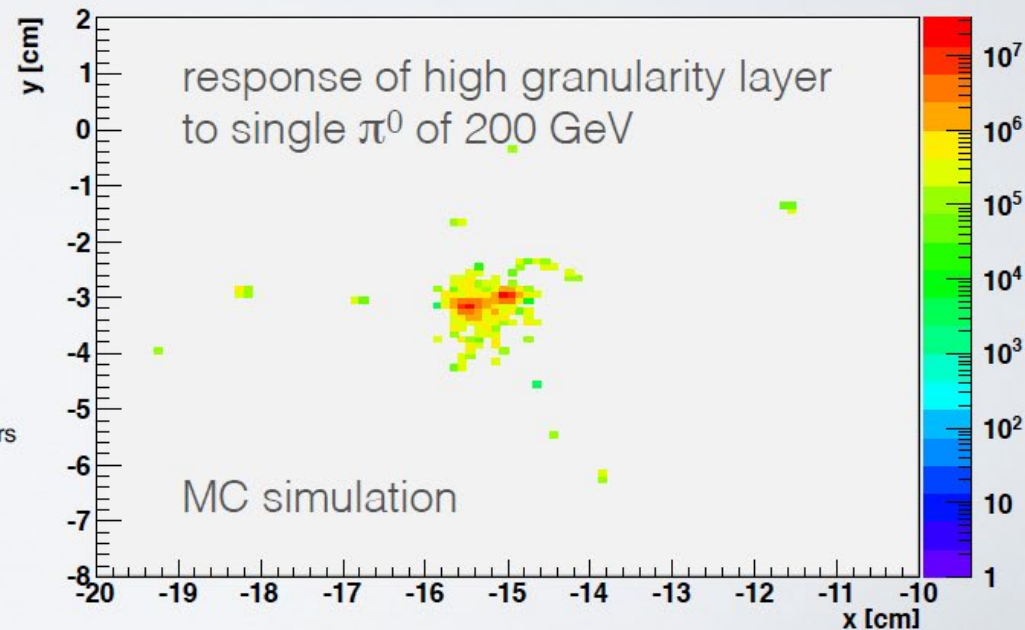


studied in performance simulations:

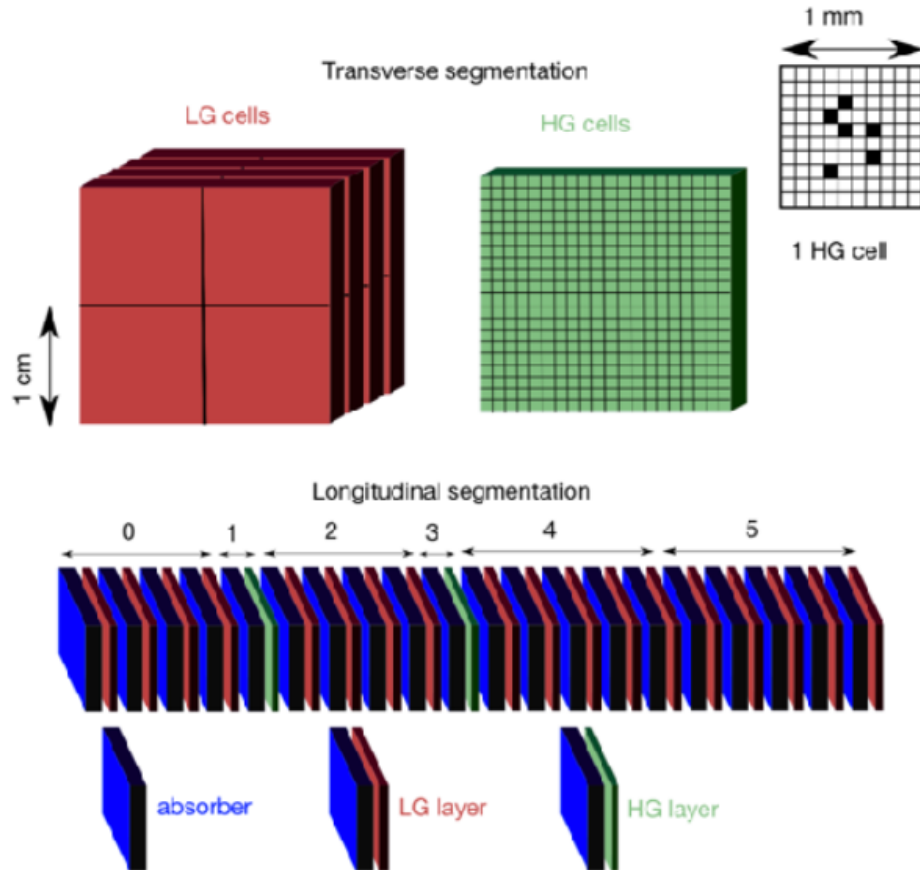
24 layers:

W ( $3.5\text{mm} \approx 1 X_0$ ) + Si-sensors (2 types)

- low granularity ( $\approx 1\text{ cm}^2$ ), Si-pads
- high granularity ( $\approx 1\text{ mm}^2$ ), obtained with pixels (e.g. CMOS-MAPS)



# FoCal-E design



Studied in simulations 20 layers:  
 $W(3.5 \text{ mm} \approx 1X_0)$  + silicon sensors  
 Two types: Pads (LG) and Pixels (HG)

- Pad layers provide shower profile and total energy
- Pixel layers provide position resolution to resolve overlapping showers

Optimizations in progress:

- Number of pixel layers and location
- Number of pad layers
- Maximum separation between layers

- Main challenge: Separate  $\gamma/\pi^0$  at high energy
  - Two photon separation from  $\pi^0$  decay ( $p_T=10 \text{ GeV}$ ,  $\eta=4.5$ )  $\sim 5\text{mm}$
  - Requires small Molière radius and high granularity readout
  - Si-W calorimeter with effective granularity  $\approx 1\text{mm}^2$

# Rapidity coverage and efficiency

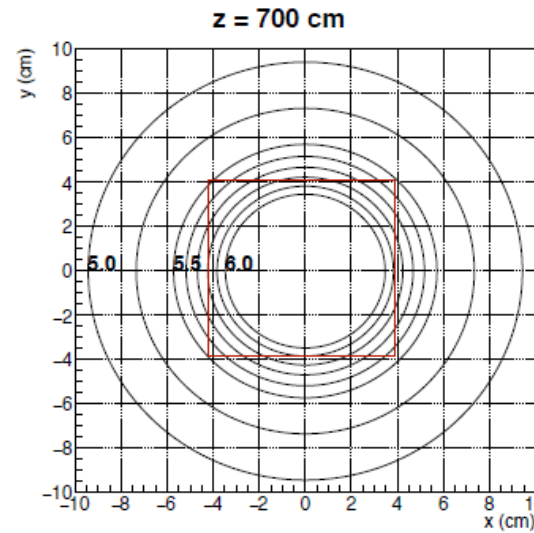
position  $z = 7\text{m}$

beam pipe radius  $3.5\text{cm}$

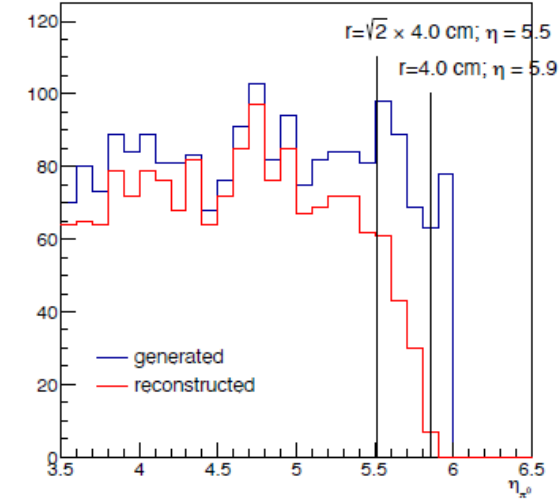
8x8cm square around beam:  
**maximum rapidity 5.5-5.8**

2-gamma distance gets small  
 beyond  $\eta=5.5$ :

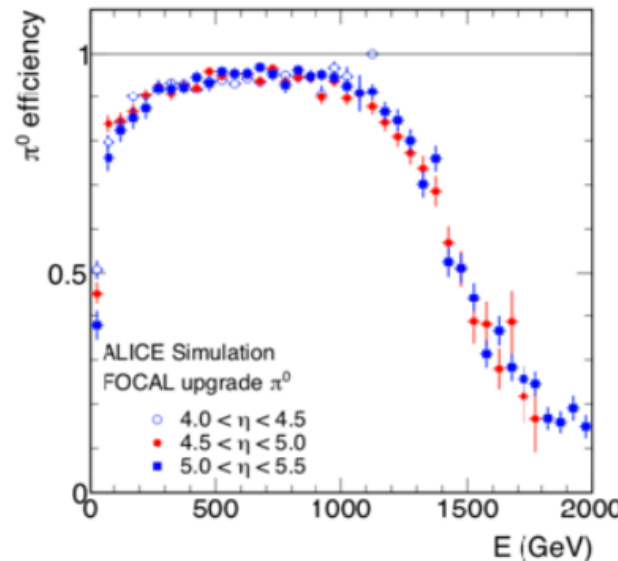
→ sharp drop at  $R_{\min}$  plus effect  
 of circle vs square



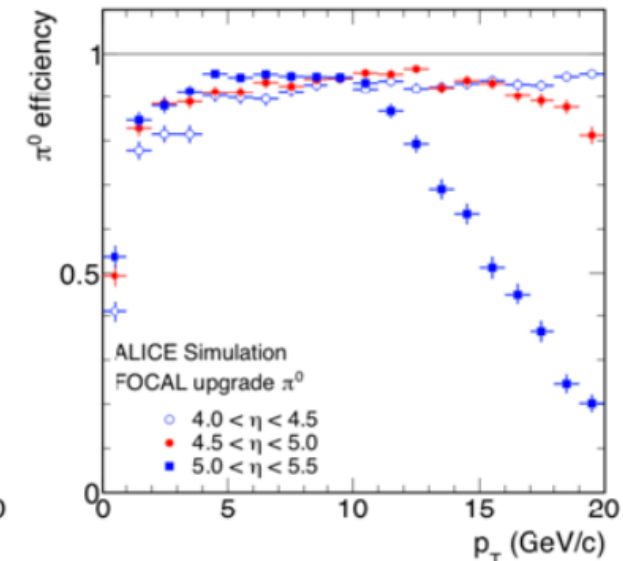
$\pi^0$  rapidity distribution



Single  $\pi^0$  efficiency vs E



Single  $\pi^0$  efficiency vs  $p_T$



Very good  $\pi^0$  efficiency  
 up to  $\eta = 5.5$   
 (falls off above  $p_T = 10\text{ GeV}$   
 due to 2-gamma distance)